Hindawi Publishing Corporation
International Journal of Antennas and Propagation
Volume 2014, Article ID 573615, 9 pages
http://dx.doi.org/10.1155/2014/573615

Research Article

Validation of the α-μ Model of the Power Spectral Density of GPS Ionospheric Amplitude Scintillation

Kelias Oliveira,[1] Alison de Oliveira Moraes,[2,3] Emanoel Costa,[4] Marcio Tadeu de Assis Honorato Muella,[5] Eurico Rodrigues de Paula,[6] and Waldecir Perrella[3]

[1]*Instituto Federal de Educação, Ciência e Tecnologia de Goiás (IFG), Goiânia, GO, Brazil*
[2]*Instituto de Aeronáutica e Espaço (IAE), São José dos Campos, SP, Brazil*
[3]*Instituto Tecnológico de Aeronáutica (ITA), São José dos Campos, SP, Brazil*
[4]*Centro de Estudos em Telecomunicações, Pontifícia Universidade Católica do Rio de Janeiro (CETUC/PUC-Rio), Rio de Janeiro, RJ, Brazil*
[5]*Instituto de Pesquisa e Desenvolvimento, Universidade do Vale do Paraíba (UNIVAP), São José dos Campos, SP, Brazil*
[6]*Instituto Nacional de Pesquisas Espaciais (INPE), São José dos Campos, SP, Brazil*

Correspondence should be addressed to Alison de Oliveira Moraes; alisonaom@iae.cta.br

Received 19 September 2014; Accepted 19 November 2014; Published 23 December 2014

Academic Editor: Jit S. Mandeep

The α-μ model has become widely used in statistical analyses of radio channels, due to the flexibility provided by its two degrees of freedom. Among several applications, it has been used in the characterization of low-latitude amplitude scintillation, which frequently occurs during the nighttime of particular seasons of high solar flux years, affecting radio signals that propagate through the ionosphere. Depending on temporal and spatial distributions, ionospheric scintillation may cause availability and precision problems to users of global navigation satellite systems. The present work initially stresses the importance of the flexibility provided by α-μ model in comparison with the limitations of a single-parameter distribution for the representation of first-order statistics of amplitude scintillation. Next, it focuses on the statistical evaluation of the power spectral density of ionospheric amplitude scintillation. The formulation based on the α-μ model is developed and validated using experimental data obtained in São José dos Campos (23.1°S; 45.8°W; dip latitude 17.3°S), Brazil, located near the southern crest of the ionospheric equatorial ionization anomaly. These data were collected between December 2001 and January 2002, a period of high solar flux conditions. The results show that the proposed model fits power spectral densities estimated from field data quite well.

1. Introduction

The presence of random irregularities in the ionospheric plasma density may cause amplitude and phase scintillation on signals of the global navigation satellite systems (GNSS). These effects may be strong enough to cause cycle slips, loss of signal tracking, and, consequently, degradation in the performance and positioning accuracy of ground-based receivers. Thus, all technological infrastructures that depend on GNSS signals for precise positioning and navigation can be directly affected.

Ionospheric scintillation at GNSS frequencies is a phenomenon that typically occurs after sunset and mainly during premidnight hours. Its occurrence is predominant at the polar and low-latitude regions. The present contribution will focus on scintillation which occurs within the latitude belt of ±20° centered at the geomagnetic equator. Climatological studies of equatorial and low-latitude ionospheric scintillation have shown combined seasonal and longitudinal dependence. For example, in the Brazilian longitudinal sector, the ionospheric irregularity activity is more intense near December solstice months [1]. This behavior departs from that in the western sector of South America, where the scintillation occurrence peaks during the equinoctial period. These studies also indicated that scintillation is more intense during

solar maximum years (when the ionospheric layer is thicker and denser).

Adequate knowledge of the temporal properties and fading time scales of amplitude scintillation can be very useful in the development of appropriated mitigation tools of current positioning/navigation applications based on GNSS signals. Fremouw et al. [2] demonstrated that Nakagami-m probability density function (PDF) describes well the variability of the amplitude scintillations. Later, Hegarty et al. [3] developed an amplitude scintillation signal model based on a Nakagami-m distribution. In [4] it was presented that either the Nakagami-m or the Rice PDF could describe well the distribution of amplitudes that were present in their measurements. More recently, Moraes et al. [5] showed that the ionospheric amplitude scintillation phenomenon can be modeled by using first-order statistics of the α-μ distribution proposed by Yacoub [6]. Moraes et al. [7] also represented the level crossing rate (LCR) and average fading duration (AFD) due to equatorial ionospheric scintillation using the same distribution. This model explores the nonlinearity of the propagation medium, associating the physical fading phenomena with the α and μ parameters. Moraes et al. [5, 7] empirically tested and parameterized this distribution as a function of scintillation severity, showing that this model provides a better fit to experimental data than those yielded by previous ones. Indeed, having two parameters that are physically described, instead of just one as in the previous fading models (such as those based on the Nakagami-m distribution), makes the α-μ distribution more flexible, assuring a better agreement with scintillation data. Additionally, they proposed a series of approximations to the estimation of the α and μ parameters tailored to the severity of the ionospheric scintillation events.

In the communications field, the power spectral density (PSD) of the random refractive-index fluctuations in the propagation medium is an important feature for channel characterizations and performance evaluations. PSD characteristics are directly related to size, behavior, speed, and duration of ionospheric irregularities [8–10]. The PSD is widely used to study and model the ionospheric plasma irregularity processes. For example, by using these PSDs, it is possible to estimate the drift velocity and the average height of the irregularities in the ionosphere. The literature also lists a substantial number of works dealing with the PSDs of VHF and UHF transionospheric signals [11–15]. The temporal variations in the received signal caused by the ionosphere have been analyzed using PSD models by many works in the literature [4, 16, 17]. The spectrum widths of received signals affected by scintillation provide important information that may be considered in the design of the bandwidths of tracking loops of GNSS receivers [16].

In continuation of previous work by Moraes et al. [5, 7, 18], the present study presents the experimental validation of the α-μ model for the PSD of transionospheric signals received on the ground, by comparing results from the formulation of Dias and Yacoub [19] with those from real scintillation data.

The remainder of the present paper is organized in the following way. Section 2 describes the measurements and the initial processing of the data to estimate some fundamental parameters. Section 3 summarizes the benefits of the first-order statistical characterization of scintillation using the α-μ distribution. Section 4 discusses the power spectral density formulation based on the α-μ distribution and presents the obtained results from the model validation. Finally, Section 5 presents concluding remarks.

2. Measurements

The scintillation monitor (SCINTMON) used in the campaign was developed at Cornell University [20] with a 12-channel correlator and built using a GEC-Plessey GPS card with special firmware, which was designed to maintain lock even under extreme scintillation scenarios. The monitor tracks signals from up to 11 GPS satellites, simultaneously. One channel is dedicated to noise floor estimation. Its front end works on the L1 band (1575.42 MHz) and provides measurements of wide band power and wide band noise with a 50 Hz sampling rate. Unfortunately, SCINTMON does not provide carrier phase measurements. More information about SCINTMON can be found in [21].

The scintillation monitor was installed at the Instituto Nacional de Pesquisas Espaciais (INPE) headquarters in São José dos Campos (SJC), Brazil (geographic coordinates: 23.2°S, 45.9°W, dip latitude: 17.5°S), near the southern peaks of the equatorial anomaly, where the world's strongest scintillation occurs during high solar flux years. The measurements were made between December 14, 2001, and January 14, 2002. During this period, the average sunspot number and the 10.7 cm solar flux density were 126 and 176×10^{-22} W/m^2/Hz, respectively. This period is part of the equatorial spread F season in Brazil, which starts around September and lasts until April [22]. Scintillation observations started at 18:00 LT and continued until the next day at 06:00 LT. Scintillation at GHz frequencies is normally observed between sunset hours and local midnight, but cases of postmidnight scintillation have also been observed. In this study, only data from GPS satellites with elevation greater than 30° were considered, to avoid signal contamination by nongeophysical sources (such as tropospheric scattering and multipath). The geophysical conditions under which the measurements were made allow the study of broad range of scintillation levels. From the set of observations (over 370 hours during 32 days of measurements), approximately 102 hours of significant GPS L1 amplitude scintillation were obtained.

In Figure 1(a), the measurement site SJC is overlaid on the global map of the predicted maximum electron density (NmF2) of the ionosphere at 20:00 LT on December 31, 2001 (day of the year DOY = 365). This map, generated using the international reference ionosphere (IRI) model [23], clearly shows the enhancement of NmF2 in the equatorial anomaly region. Indeed, strong scintillation is known to occur more frequently during high solar flux conditions than during moderate or low solar flux conditions [24]. Figure 1(b) shows the azimuth-elevation track of satellite PRN 18 over SJC during the evening hours on December 15, 2001. The scintillation index S_4 will be defined in the next section. The time series of the ratio C/N_o (dBHz) between the received power and the noise power density corresponding to the link characterized

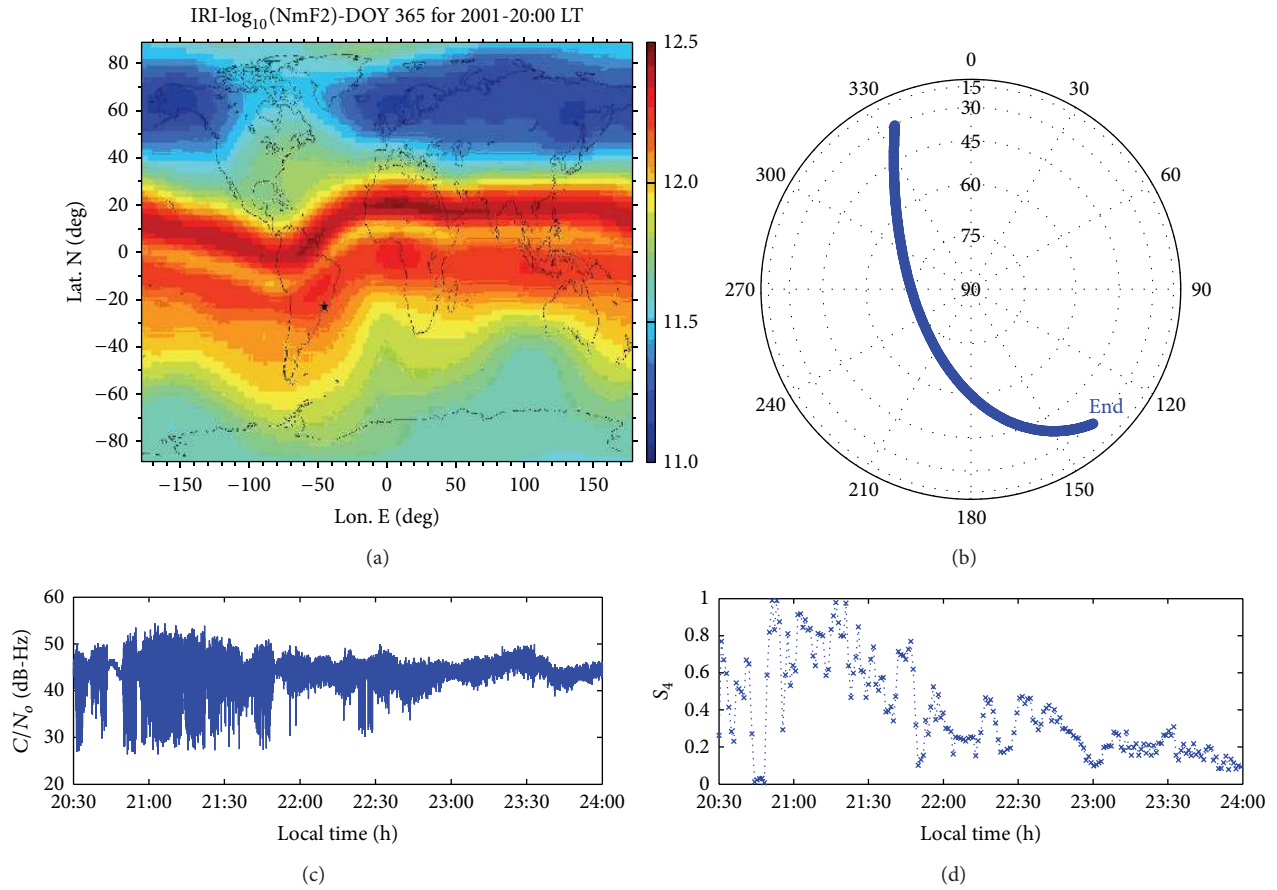

FIGURE 1: (a) The location of the measurement site SJC overlaid on the global map of the predicted ionospheric maximum electron density (NmF2) at 20:00 LT on December 31, 2001. This map was generated using the international reference ionosphere (IRI) model [26]. (b) Skyplot of satellite PRN 18 on December 15, 2001. (c) Ratio C/N_o (dBHz) between the received power and the noise power density corresponding to the link characterized by panel (b). (d) Respective scintillation index S_4 for consecutive one-minute records of C/N_o (3000 samples).

by Figure 1(b) is shown in Figure 1(c), respectively. Additional details about the selected datasets and their preprocessing can be found in Moraes et al. [25].

2.1. Processing of the Scintillation Data. The strength of the amplitude scintillation is characterized by the index S_4, defined as the normalized standard deviation of the received signal intensity (power). That is, it is given by [26]

$$S_4 = \sqrt{\frac{\langle I^2 \rangle - \langle I \rangle^2}{\langle I \rangle^2}}, \tag{1}$$

where $I = |R|^2$ is the intensity, R is the amplitude of received signal, and the angular brackets denote an ensemble average (time average of one-minute records).

The S_4 index is computed by SCINTIMON using the wide band power P and noise wide band power N measurements, as well as their respective low-pass filtered versions $\langle P \rangle$ and $\langle N \rangle$ in a slightly less straightforward way. The filtered versions are obtained using a 6th order low-pass Butterworth filter with a cutoff frequency of 0.1 Hz [21]. The series of P and $\langle P \rangle$ are then used to estimate the real signal strength variance over a one-minute period following the approach described by [21]:

$$\widehat{\sigma}^2 = \frac{1}{M} \sum_{k=1}^{M} \left(P_k - \langle P \rangle_k \right) \left(P_{k-1} - \langle P \rangle_{k-1} \right), \tag{2}$$

where $M = 3000$ is the total number of samples during each 60-second period. The respective mean signal power ($\widehat{S}$) is given by

$$\widehat{S} = \frac{1}{M} \sum_{k=1}^{M} \left(\langle P \rangle_k - \langle N \rangle_k \right). \tag{3}$$

The computed S_4 index is finally given by

$$S_4 = \sqrt{\frac{\widehat{\sigma}^2}{\widehat{S}}}. \tag{4}$$

Figure 1(d) shows the results from the calculations of the scintillation index S_4 for every one-minute record of the signal displayed in Figure 1(c).

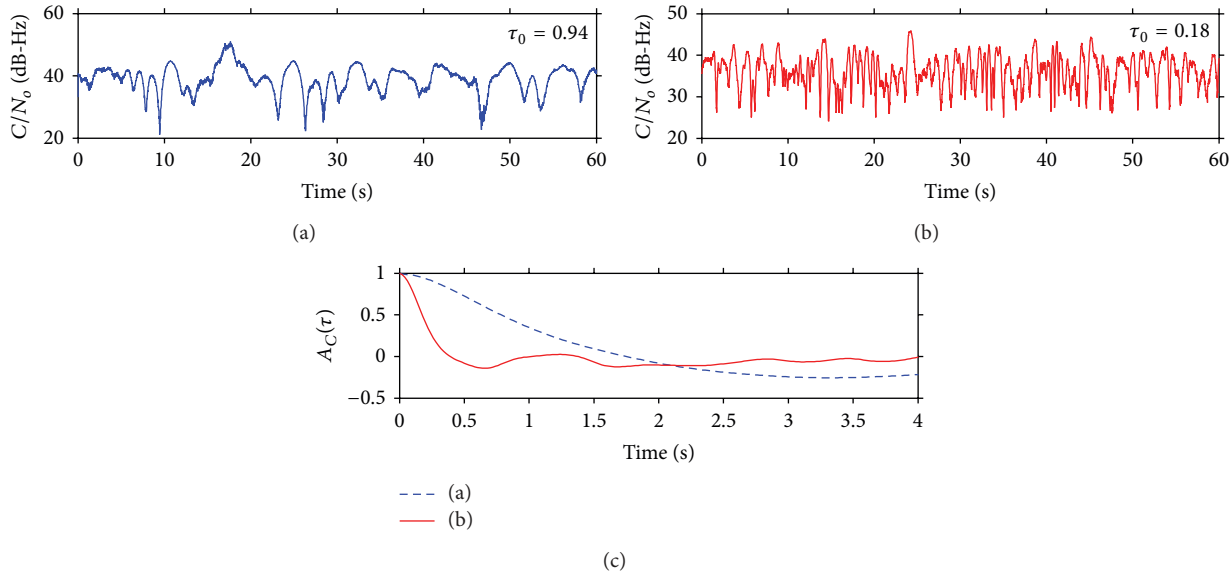

FIGURE 2: ((a) and (b)) Two examples of scintillation observations with $S_4 = 0.9$ but with different decorrelation times τ_0. (c) Autocorrelation coefficients for (a) and (b) cases, respectively.

Additionally, the normalized signal amplitude scintillation (R) is obtained by [23]

$$R = \sqrt{\frac{P}{\langle P\rangle - \langle N\rangle}}. \tag{5}$$

The autocorrelation coefficient of the normalized signal amplitude scintillation $A_C(\tau)$ is given by

$$A_C(\tau) = \frac{E\left[\left(R(t) - z\right)\left(R(t+\tau) - z\right)\right]}{{\sigma_A}^2}, \tag{6}$$

where $E[]$ denotes the expected value operator (again implemented by a time average) and z and σ_A are the mean and variance values of R. Another important parameter used to characterize scintillation is the decorrelation time τ_0, defined as the time lag at which the autocorrelation function falls off by e^{-1} from its maximum (zero lag) value [4]:

$$\frac{A_C(\tau_0)}{A_C(0)} = e^{-1}. \tag{7}$$

While the S_4 index is an indicator of the strength of amplitude fading, the decorrelation time τ_0 is an indicator of the rapidity of the fades.

The two examples in Figures 2(a) and 2(b) illustrate the variability in the amplitude scintillation patterns and the decorrelation time estimated from the measurements made during the campaign. The two cases display approximately the same S_4 index (0.9), but very distinct τ_0 values, 0.94 s and 0.18 s, respectively. Figure 2(c) shows the respective autocorrelation coefficients, $A_C(\tau)$, for both cases and as consequence their temporal differences.

3. The α-μ Model for Scintillation

The α-μ distribution is a general fading model proposed by Yacoub [6]. The use of this distribution for modeling ionospheric amplitude scintillation was proposed by Moraes et al. [5]. Assuming that the average signal intensity r^2 is equal to one, the α-μ probability density function of the normalized amplitude envelope r of the received signal is given by

$$f(r) = \frac{\alpha r^{\alpha\mu-1}}{\xi^{\alpha\mu/2}\Gamma(\mu)} \exp\left(-\frac{r^\alpha}{\xi^{\alpha/2}}\right), \quad \xi = \frac{\Gamma(\mu)}{\Gamma(\mu + 2/\alpha)}, \tag{8}$$

where $\Gamma(x)$ is the Gamma function of the argument x.

The α-μ parameters can be estimated based on the equality that involves the moments of α-μ envelope given by

$$\frac{E^2\left(r^\beta\right)}{E\left(r^{2\beta}\right) - E^2\left(r^\beta\right)} = \frac{\Gamma^2(\mu + \beta/\alpha)}{\Gamma(\mu)\Gamma(\mu + 2\beta/\alpha) - \Gamma^2(\mu + \beta/\alpha)}. \tag{9}$$

As suggested by Yacoub [6], the left hand side of (9) can be obtained from field data for arbitrarily selected values of β. Assuming, for instance, $\beta = 1$ and $\beta = 2$, a system with two nonlinear equations for the two desired unknowns α and μ is established and can be solved. This is the ideal approach when real data are available. Alternatively, assuming $\beta = 2$ in (9) and combining the result with (1), it is possible to establish the following relation between the scintillation index S_4 and the parameters of the α-μ distribution:

$${S_4}^2 = \frac{\Gamma(\mu)\Gamma(\mu + 4/\alpha) - \Gamma^2(\mu + 2/\alpha)}{\Gamma^2(\mu + 2/\alpha)}. \tag{10}$$

The single-parameter Nakagami-m distribution has been used for a long time as the model that best described the amplitude scintillation phenomenon [2, 16]. It can be

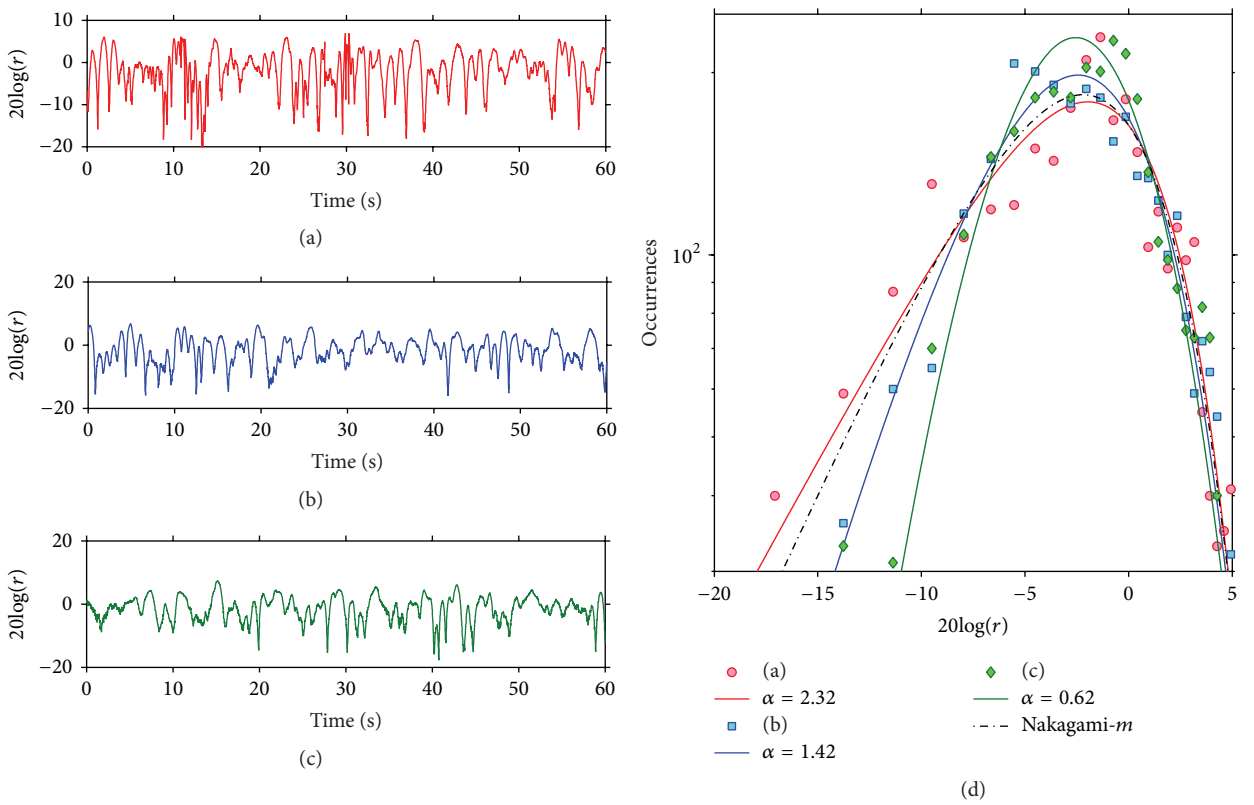

FIGURE 3: ((a), (b), and (c)) Three cases illustrating different scintillation patterns with approximately the same scintillation index S_4 (≈0.90). (d) Corresponding measured and calculated α-μ distributions with parameters estimated with basis on (9), as well as the Nakagami-m distribution with $m = 1/0.9^2 = 1.23$.

obtained from the α-μ distribution with $\alpha = 2$ and $\mu = m = 1/{S_4}^2$. Note that each value of the scintillation index S_4 provides a unique Nakagami-m distribution. However, there are an infinite number of α and μ values that satisfy (10) for each value of S_4. Equation (10) is convenient, because it indicates that, differently from the Nakagami-m distribution, the α-μ model may describe different patterns of scintillation for the same scintillation index S_4. This is especially interesting for strong scintillation, where the S_4 index alone is not considered a proper indication of the ionospheric perturbations. Indeed, it saturates to a value near unity under increasingly strong scattering conditions, in addition to being independent of the rate of signal fading [27].

To stress the importance of the flexibility provided by α-μ model in comparison with the limitations of the Nakagami-m distribution in this particular aspect, Figures 3(a), 3(b), and 3(c) show three examples of different scintillation patterns with approximately the same scintillation index S_4 (≈0.90). These cases, which have not been presented previously, were selected from the data base described in Section 2 [25]. Figure 3(d) displays the following: (i) the empirical PDF for each of these records, using color-coded symbols; (ii) the corresponding α-μ PDFs, with parameters estimated by the application of the procedure proposed in the text immediately following (9) to each case; and (iii) the Nakagami-m PDF (with $m = 1/0.9^2 = 1.23$). As shown in Figure 3(d), the differences among the PDFs of these received signals, captured by the α-μ model, cannot be displayed by the single-parameter distribution. Indeed, the curves in Figure 3(d) vary substantially for the same S_4 value, that is, for the same value on the left hand side of (10). This flexibility of α-μ model, resulting from the existence of two parameters instead of just one, provides the capacity of a better fit to scintillation data. It is worth mentioning that the distributions tend to spread as α increases, occupying the lower region of intensity values with higher probabilities. This means that the increased α values, for a fixed S_4 value, represent a more severe scenario for propagation, with higher occurrence of deep fading of the received signal.

4. Power Spectral Density

The exact autocorrelation function $A_R(\tau)$ for the α-μ fading signal is given by [19]

$$A_R(\tau) = E[R(\tau)R(t+\tau)] = \frac{\hat{r}^2\Gamma^2(\mu+1/\alpha)}{\mu^{2/\alpha}\Gamma^2(\mu)} F\left(\frac{-1}{\alpha}, \frac{-1}{\alpha}, \mu; A_C(\tau)\right), \quad (11)$$

where $\hat{r} = \sqrt{\Gamma(\mu)/\Gamma(\mu+2/\alpha)}\,\mu^{1/\alpha}$ for $E(R^2) = 1$; $F(a,b,c;x)$ is the Gauss hypergeometric function with parameters a, b, and c and argument x; and $A_C(\tau)$ is the temporal autocorrelation coefficient. The literature provides several models of

autocorrelation coefficients that attempt to describe different communications scenarios with their relative scattering conditions [28]. Mason [29] analyzed the model based on a second-order Butterworth filter, expressed by

$$A_C(\tau) = \exp^{(-\beta|\tau|/\tau_0)}\left[\cos\left(\frac{\beta\tau}{\tau_0}\right) + \sin\left(\frac{\beta|\tau|}{\tau_0}\right)\right], \quad (12)$$

where $\beta \approx 1.2396464$ and τ_0 is the decorrelation time lag [4].

The power spectral density $S_R(f)$ for the α-μ envelope R is the Fourier transform of (11). According to Dias and Yacoub [19], a closed-form expression for the PSD of the α-μ envelope does not seem to exist. As a consequence, they proposed and validated the following approximation for (11) that only retains the first two lowest-order terms of the series expansion of the Gauss hypergeometric function [30]:

$$A_R(\tau) \approx \frac{\widehat{r}^2\Gamma^2(\mu + 1/\alpha)}{\mu^{2/\alpha}\Gamma^2(\mu)}\left(1 + \frac{A_C(\tau)}{\alpha^2\mu}\right). \quad (13)$$

By taking the Fourier transform of (13), the PSD $S_R(f)$ can be written as

$$S_R(f) \approx \frac{\widehat{r}^2\Gamma^2(\mu + 1/\alpha)}{\mu^{2/\alpha}\Gamma^2(\mu)}\left(\delta(f) + \frac{H(f)}{\alpha^2\mu}\right), \quad (14)$$

where $\delta(x)$ is the Dirac delta function and $H(f)$ is the Fourier transform of the autocorrelation coefficients $A_C(\tau)$. It is important to note that (14) is transformed into the Nakagami-m PSD of Dias et al. [31] for $\alpha = 2$. Analyses of a limited set of representations for $A_C(\tau)$ by Humphreys et al. [4] and Moraes et al. [32] performed in the frequency and time domains, respectively, verified that the Butterworth model provided the best spectral shape for ionospheric scintillation studies. The second-order Butterworth PSD is expressed by

$$H(f) = \frac{2\tau_o/\beta}{1 + (f/f_o)^{2p}}, \quad (15)$$

where $f_o = \beta/(\sqrt{2}\pi\tau_0)$ is the 3 dB cutoff frequency and $p = 2$ is the slope factor [4]. Figure 4 shows three examples of the Nakagami-m (dashed lines) and α-μ (solid lines) PSDs represented by (14), for different values of the scintillation index S_4, assuming $\tau_o = 0.47$ s and thus $f_o = 0.59$ Hz. More information on τ_o and its typical values can be found in Moraes et al. [25].

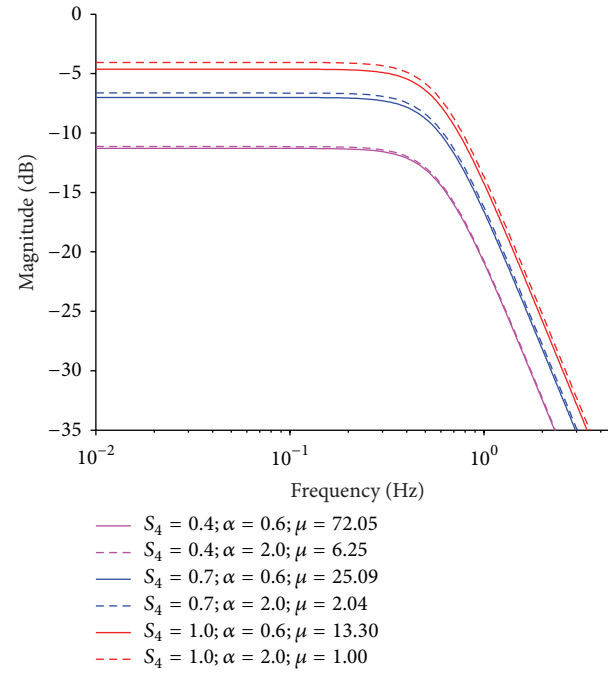

Figure 4: Nakagami-m (dashed) and α-μ (solid) PSDs for $S_4 = 0.4$, 0.7, and 1.0. The α-μ examples assume the approximation $\alpha = 1/\log(10S_4)$ and determine μ from (10).

5. Validation

In this section, the α-μ power spectral density formulation represented by (14) is compared with corresponding estimations from one-minute records of real scintillation data using the well-known Welch method [33].

For calculations, the decorrelation time lag τ_o, which is the basic parameter of (15), is determined from the estimated autocorrelation coefficient $A_C(\tau)$ according to (6). The values of S_4, α, and μ are estimated for each one-minute record as explained in Sections 2 and 3. The metric adopted by the validation of the power spectral density formulation is based on Carrano et al. [34], defined by

$$\upsilon = \frac{1}{f_{\max} - f_{\min}}\int_{f_{\min}}^{f_{\max}}\left[\log S_R(f) - \log \widehat{S}_R(f)\right]^2 df, \quad (16)$$

where $\widehat{S}_R(f)$ is the estimated PSD and $S_R(f)$ is obtained from (14) and (15). Only the sections of the power spectral density located between $f_{\min} = 0.1$ Hz and $f_{\max} = 3.0$ Hz are used in the comparison. The value for $f_{\min}$ was chosen with basis on the cutoff frequency of 0.1 Hz, according to the scintillation processing described in Section 2.1 [21]. The value for $f_{\max}$ was selected to avoid any possible contamination of the results from the analysis by the noise floor of the estimated PSDs.

Figure 5 shows examples of empirical and α-μ PSDs for different values of S_4. Figure 6 displays two additional examples that also include the results from the Nakagami-m formulation. A good agreement between empirical and calculated spectra is observed in all cases for $f \le f_{\max}$, both visually and by the small values obtained for the parameter υ. This agreement is kept until the noise-dominated frequency band is reached. It is interesting to observe in Figure 6 that the differences between the two formulations are small. Note that only the positive halves of the empirical and calculated spectra have been plotted, since they are symmetrical around zero. However, all the PSD values corresponding to nonzero frequencies have been multiplied by two, to conserve the full power of the spectra. This procedure does not affect the calculations indicated by (16).

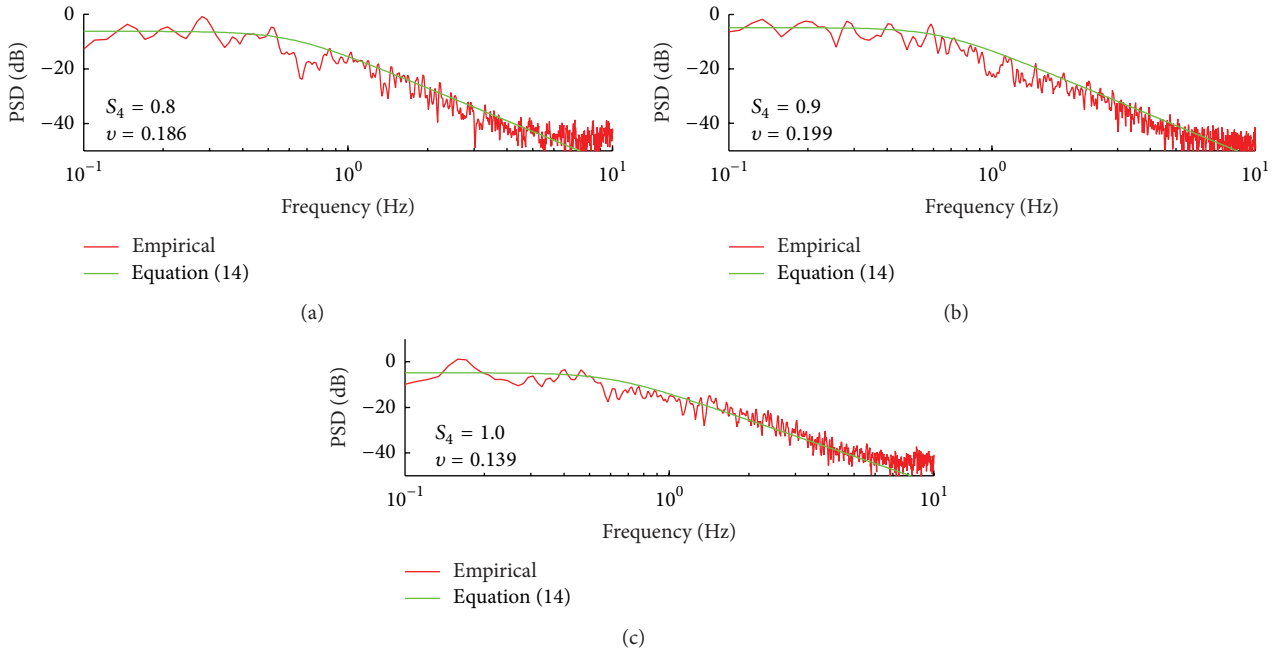

Figure 5: Estimated scintillation power spectral densities (red) and corresponding results (green) from the theoretical α-μ formulation represented by (14) for different values of the scintillation index S_4.

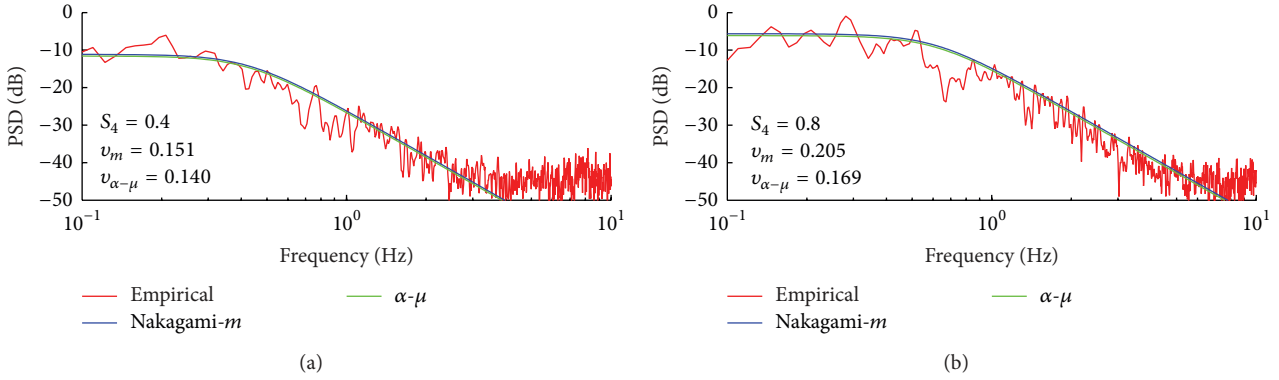

Figure 6: Comparison between estimated scintillation power spectral densities (red) and corresponding results from the theoretical α-μ (green) and Nakagami-m (blue) formulations for different values of the scintillation index S_4.

The results from the application of the validation procedure to the full data set are summarized in Table 1. The second line of the table displays the number of one-minute records in each of the classes of scintillation index $0.1n - 0.025 < S_4 < 0.1n + 0.025$ ($n = 3, \ldots, 10$). In the next two lines, Table 1 displays the average error parameter υ for the α-μ and Nakagami-m formulations, which are larger than the ones displayed in Figures 5 and 6 for all classes of S_4. It is observed that, on average, the α-μ formulation provides slightly better fits to empirical PSDs than those provided by the Nakagami-m model. This result was expected from the discussion in Section 3 and the studies of the second-order statistics of level crossing rate (LCR) and average fading duration (AFD) presented by Moraes et al. [5, 7]. Additionally, this table also shows the average values of the cutoff frequency f_o and $1/\tau_0$ frequency for each class of scintillation index. The spectral broadening as S_4 increases, previously observed by other authors [16], is evident in the last two lines of Table 1.

Another important result from the above analysis is the performance of Nakagami-m spectrum formulation in comparison with that of the α-μ model. During the validation process, it was noted that the difference between both spectra is less than 1 dB. For spectral analysis purposes only, without taking first-order statistics considerations into account, the Nakagami-m model proved to be fairly accurate.

6. Concluding Remarks

The ionosphere is known to affect Earth-space communications and GNSS applications operating in the L band and below. One of the effects on transionospheric radio waves is associated with amplitude scintillation caused by the presence

Table 1: Error results for the validation of the power spectral density formulation.

$S_4 \pm 0.025$	0.3	0.4	0.5	0.6	0.7	0.8	0.9	1.0
Cases (min)	1423	742	526	338	243	161	111	44
$E[\upsilon_{\alpha-\mu}]$	0.337	0.292	0.297	0.290	0.320	0.306	0.277	0.255
$E[\upsilon_m]$	0.327	0.297	0.314	0.314	0.344	0.324	0.296	0.281
$E[1/\tau_0]$ (Hz)	1.40	1.52	1.69	1.90	2.16	2.51	2.91	3.15
$E[f_o]$ (Hz)	0.39	0.42	0.47	0.53	0.60	0.70	0.81	0.87

of random plasma density irregularities. Thus, it is important to develop increasingly accurate statistical models to describe the temporal properties of amplitude scintillation.

The present work initially stressed the importance of the flexibility provided by α-μ model in comparison with the limitations of the Nakagami-m distribution for the representation of first-order statistics of scintillation.

Next, the α-μ and its special case, Nakagami-m, were validated for second-order statistics of amplitude scintillation by comparison of the associated power spectral density formulations with estimations from real data. The validation results show that the characterizations of the PSD of amplitude scintillation by both models are in good agreement with the experimental estimates. The α-μ model is marginally better than that provided by the Nakagami-m formulation. However, it should be observed that these models may be highly dependent on the assumed autocorrelation coefficient model.

Conflict of Interests

The authors declare that there is no conflict of interests regarding the publication of this paper.

Acknowledgments

The authors are grateful to Professor Fabiano Rodrigues (University of Texas at Dallas, TX, USA) for the discussions concerning the application of the α-μ model for scintillation. Kelias Oliveira is grateful to Instituto Federal de Educação, Ciência e Tecnologia de Goiás, for supporting his doctoral studies at ITA through Award DINTER ITA/IFG 23038.044846/2009-76. Alison de Oliveira Moraes wishes to thank Instituto de Aeronáutica e Espaço (IAE), where he works as a Research Engineer, for assisting his cooperation research with ICEA, INPE, and ITA. Emanoel Costa was supported by AFOSR Award FA9550-12-1-0031 during the present work. Eurico Rodrigues de Paula is grateful for the partial supports from AFOSR FA9550-10-1-0564 and Conselho Nacional de Desenvolvimento Científico e Tecnológico (CNPq) 305684/2010-8 Grants. Marcio Tadeu de Assis Honorato Muella would like to thank the support from CNPq under Process no. 308017/2011-0.

References

[1] M. A. Abdu, J. H. A. Sobral, I. S. Batista, V. H. Rios, and C. Medina, "Equatorial spread-F occurence statistics in the American longitudes: diurnal, seasonal and solar cycle variations," *Advances in Space Research*, vol. 22, no. 6, pp. 851–854, 1998.

[2] E. J. Fremouw, R. C. Livingston, and D. A. Miller, "On the statistics of scintillating signals," *Journal of Atmospheric and Terrestrial Physics*, vol. 42, pp. 717–731, 1980.

[3] C. Hegarty, M. B. El-Arini, T. Kim, and S. Ericson, "Scintillation modeling for GPS-wide area augmentation system receivers," *Radio Science*, vol. 36, no. 5, pp. 1221–1231, 2001.

[4] T. E. Humphreys, M. L. Psiaki, J. C. Hinks, B. O'Hanlon, and P. M. Kintner Jr., "Simulating ionosphere-induced scintillation for testing GPS receiver phase tracking loops," *IEEE Journal on Selected Topics in Signal Processing*, vol. 3, no. 4, pp. 707–715, 2009.

[5] A. O. Moraes, E. R. de Paula, W. J. Perrella, and F. S. Rodrigues, "On the distribution of GPS signal amplitudes during low-latitude ionospheric scintillation," *GPS Solutions*, vol. 17, no. 4, pp. 499–510, 2013.

[6] M. D. Yacoub, "The α-μ distribution: a physical fading model for the Stacy distribution," *IEEE Transactions on Vehicular Technology*, vol. 56, no. 1, pp. 27–34, 2007.

[7] A. O. Moraes, E. R. de Paula, M. T. A. H. Muella, and W. J. Perrella, "On the second order statistics for GPS ionospheric scintillation modeling," *Radio Science*, vol. 49, no. 2, pp. 94–105, 2014.

[8] A. Bhattacharyya, K. C. Yeh, and S. J. Franke, "Deducing turbulence parameters from transionospheric scintillation measurements," *Space Science Reviews*, vol. 61, no. 3-4, pp. 335–386, 1992.

[9] P. M. Kintner, H. Kil, T. L. Beach, and E. R. de Paula, "Fading timescales associated with GPS signals and potential consequences," *Radio Science*, vol. 36, no. 4, pp. 731–743, 2001.

[10] K. N. Iyer, M. N. Jivani, M. A. Abdu, H. P. Joshi, and M. Aggarwal, "Power spectral studies of VHF ionospheric scintillations near the crest of the equatorial anomaly in India," *Indian Journal of Radio & Space Physics*, vol. 35, no. 4, pp. 234–241, 2006.

[11] C. L. Rufenach, "Power-law wavenumber spectrum deduced from ionospheric scintillation observations," *Journal of Geophysical Research*, vol. 77, no. 25, pp. 4761–4772, 1972.

[12] R. K. Crane, "Spectra of ionospheric scintillation," *Journal of Geophysical Research*, vol. 81, no. 13, pp. 2041–2050, 1976.

[13] R. Umeki, C. H. Liu, and K. C. Yeh, "Multifrequency spectra of ionospheric amplitude scintillation," *Journal of Geophysical Research*, vol. 82, no. 19, pp. 2752–2760, 1977.

[14] C. L. Rino, "On the application of phase screen models to the interpretation of ionospheric scintillation data," *Radio Science*, vol. 17, no. 4, pp. 855–867, 1982.

[15] H. J. Strangeways, Y.-H. Ho, M. H. O. Aquino et al., "On determining spectral parameters, tracking jitter, and GPS positioning improvement by scintillation mitigation," *Radio Science*, vol. 46, no. 6, 2011.

[16] P. K. Banerjee, R. S. Dabas, and B. M. Reddy, "C and L band transionospheric scintillation experiment. Some results for applications to satellite radio systems," *Radio Science*, vol. 27, no. 6, pp. 955–969, 1992.

[17] R. A. Dana, "Effects of ionospheric scintillation on differential demodulation of GPS data," *IEEE Transactions on Aerospace and Electronic Systems*, vol. 33, no. 3, pp. 893–902, 1997.

[18] A. O. Moraes, E. Costa, E. R. de Paula, W. J. Perrella, and J. F. G. Monico, "Extended ionospheric amplitude scintillation model for GPS receivers," *Radio Science*, vol. 49, no. 5, pp. 315–329, 2014.

[19] U. S. Dias and M. D. Yacoub, "On the α-μ autocorrelation and power spectrum functions: field trials and validation," in *Proceedings of the IEEE Global Telecommunications Conference (GLOBECOM '09)*, pp. 1–6, IEEE, Honolulu, Hawaii, USA, December 2009.

[20] T. L. Beach and P. M. Kintner, "Development and use of a GPS ionospheric scintillation monitor," *IEEE Transactions on Geoscience and Remote Sensing*, vol. 39, no. 5, pp. 918–928, 2001.

[21] T. L. Beach, *Global positioning system studies of equatorial scintillations [Ph.D. thesis]*, Cornell University, 1998.

[22] J. H. A. Sobral, M. A. Abdu, H. Takahashi et al., "Ionospheric plasma bubble climatology over Brazil based on 22 years (1977–1998) of 630 nm airglow observations," *Journal of Atmospheric and Solar-Terrestrial Physics*, vol. 64, no. 12–14, pp. 1517–1524, 2002.

[23] D. Bilitza, "35 years of international reference ionosphere—Karl Rawer's legacy," *Advances in Radio Science*, vol. 2, pp. 283–287, 2004.

[24] J. Aarons, "Global morphology of ionospheric scintillations," *Proceedings of the IEEE*, vol. 70, no. 4, pp. 360–378, 1982.

[25] A. O. Moraes, F. S. da Rodrigues, W. J. Perrella, and E. R. de Paula, "Analysis of the characteristics of low-latitude GPS amplitude scintillation measured during solar maximum conditions and implications for receiver performance," *Surveys in Geophysics*, vol. 33, no. 5, pp. 1107–1131, 2012.

[26] B. H. Briggs and I. A. Parkin, "On the variation of radio star and satellite scintillations with zenith angle," *Journal of Atmospheric and Terrestrial Physics*, vol. 25, no. 6, pp. 339–366, 1963.

[27] C. S. Carrano and K. M. Groves, "Temporal decorrelation of GPS satellite signals due to multiple scattering from ionospheric irregularities," in *Proceedings of the 23rd International Technical Meeting of the Satellite Division of the Institute of Navigation (ION GNSS '10)*, pp. 361–374, Portland, Ore, USA, September 2010.

[28] M. K. Simon and M. S. Alouini, *Digital Communication Over Fading Channels*, Wiley-Interscience, 2nd edition, 2006.

[29] L. J. Mason, "Error probability evaluation for systems employing differential detection in a Rician fast fading environment and Gaussian noise," *IEEE Transactions on Communications*, vol. 35, no. 1, pp. 39–46, 1987.

[30] M. Abramowitz and I. A. Stegun, *Handbook of Mathematical Functions*, Dover, New York, NY, USA, 1968.

[31] U. S. Dias, M. D. Yacoub, J. C. S. S. Filho, G. Fraidenraich, and D. B. da Costa, "On the Nakagami-m autocorrelation and power spectrum functions: field trials and validation," in *Proceedings of the International Telecommunications Symposium (ITS '06)*, pp. 253–256, IEEE, Fortaleza, Brazil, September 2006.

[32] A. O. Moraes, E. R. de Paula, W. J. Perrella, and E. Costa, "Investigation of autocorrelation models for ionospheric amplitude scintillation," in *Proceedings of the Beacon Satellite Symposium*, 2013.

[33] S. M. Kay, *Modern Spectral Estimation: Theory and Application*, Prentice Hall, 1988.

[34] C. S. Carrano, C. E. Valladares, and K. M. Groves, "Latitudinal and local time variation of ionospheric turbulence parameters during the conjugate point equatorial experiment in Brazil," *International Journal of Geophysics*, vol. 2012, Article ID 103963, 16 pages, 2012.